



Evaluations of Reactions Cross Section of Radionuclide by Particles Induced Nuclear Reactions using Exifon Code

I. Ahmad¹, Y. Y. Ibrahim², Koki, F.S³

¹Department of Physics, Bayero University Kano.

²Department of Physics, Bayero University Kano

³Department of Physics, Bayero University Kano

Abstract

In this work the reaction cross section for the production radionuclide of $^{208,207,206}\text{Pb}$ and $^{207,205,204}\text{Tl}$ isotopes from bismuth-208 were calculated using EXIFON code in the energy range from 0 MeV to 30 MeV. The code is based on an analytical model for statistical multistep direct and multistep compound reactions (SMD/SMC model). The results obtained shows that production of ^{207}Tl is not observed at this energy range because the interaction cross section is zero, and also the excitation functions for the production of ^{205}Tl and ^{204}Tl were obtained.

Keywords: Nuclear reaction; cross-section; Excitation function; Radioisotope; statistical multistep reaction; nuclear model.

1. Introduction

The artificially produced radioactive isotopes are important for many different applications[1]. Radioactive isotopes play an important role in the field of medical science in terms of beneficial applications in both diagnosis and therapy purposes[2].

In radioisotope production programmes, nuclear reactions data are mainly needed for optimization of production routes[3].

For the last 50 years, the International Atomic Energy Agency (IAEA) Nuclear Data Section (NDS) has been collating, compiling and reviewing nuclear data in a collection of databases and publications, aim of making these data available to a global audience to create an awareness of the wide ranging data available in support of nuclear-related applications[4]–[6].

Today, the nuclear databases are accessible online through the website provided by the IAEA Nuclear Data Section (NDS). This site offers access to tens of thousands of nuclear data sets that can be used for research, innovation, development and dissemination.

2. Theoretical backgrounds

A nuclear reaction is a process that occurs when a nuclear particle (nucleon or nucleus) gets into close contact with another. In Many cases of nuclear reaction a strong energy and momentum exchange takes place and the final products of the reaction are one, two, or more nuclear particles leaving the point of close contact in various directions. The products are mostly of a species different from the particles in the original pair. If we considered nuclear reactions of the type

$$a + X = Y + b \quad (1)$$

or, in more compact notation, $X(a, b)Y$, this is not the most general nuclear reaction. In the general case, an arbitrary number of particles may emerge. This reaction is sufficiently general to include most of the known nuclear reactions at low energy. The radiative capture process is interested, where X and a stay together to form a nucleus W while a gamma-particle is emitted:

$$a + X = W + h\nu \quad (2)$$

This might have included as a reaction of type (1), provided that the gamma- particle is considered of the same type as b particle. The probability of processes of type (1) or (2) as a function of the energy of the incident particle a in the energy and the direction of the outgoing particles is usually interested, we are interested in the whole set of reactions:

$$a + X = \begin{cases} X + a \\ X^* + a \\ Y + b \\ Z + c \\ etc \end{cases} \quad (3)$$

The first two reactions (3) are distinguished by the fact that the "projectile" a re-emerges after the reaction. The first of these represents elastic scattering: the projectile a leaves with the same energy and the target nucleus X is left in its initial state. The second reaction represents inelastic scattering: the target nucleus X is forced into an excited state X^* , and the projectile a re-emerges, but with energy lower than its initial one by the amount of the excitation energy given to the target nucleus.

2.1 Reaction Channels

All the reactions (3), except the elastic scattering, can be sub-divided again according to the quantum state of the residual nucleus and the emerging particle. The states of the nuclei can be denote by $\alpha', \beta', \gamma', \dots$, and the states of the incident or emerging particles by $\alpha'', \beta'', \gamma'', \dots$. If particles $a, b, etc.$, are elementary, states $\alpha'', \beta'', etc.$, refer to their spin orientation. We get the reactions

$$a_{\alpha''} + X_{\alpha'} = \begin{cases} X_{\alpha'^*} + a_{\alpha''} \\ X_{\alpha'} + a_{\alpha''} \\ Y_{\beta'} + b_{\beta''} \\ Z_{\gamma'} + c_{\gamma''} \\ etc \end{cases} \quad (4)$$

Here α' and α'' are states of the target nucleus and the incident particle, β' and β'' , or γ' and γ'' , can denote any quantum state of X and a or Y and b , respectively, which can be created in this reaction. The conservation laws of energy, angular momentum, and parity restrict the possible pairs of β' and β'' and α' and α'' , etc. Any such possible pair of residual nucleus and emerging particle, each in a definite quantum state, is called a reaction channel.

Channel $a_{\alpha''} + X_{\alpha'}$ is called the entrance channel or initiating channel of reaction (4).

To describe a reaction (1) in detail, one need to determine the motion of all the particles in the system (including all the component particle of X and Y) within that region. This is neither possible nor desirable. In this study we are interested only in the Probability of getting the final result $Y + b$.

2.2 Statistical multistep reaction

Statistical multistep models are very successful in describing nuclear reactions at energies up to about 100 MeV [7]. These models enable the description of direct, pre-equilibrium, and equilibrium processes in a consistent way for a wide mass number range and various reaction channels, e.g. neutrons, protons, alpha-particles, and gamma-particles.

The application of a statistical multistep model to heavy nuclei requires the consideration of fission as a competing process to particle and "gamma-ray emissions. Therefore, statistical multistep models should be extended to the fission channel.

In the statistical multistep model, the total emission spectrum of the process (a, xb) is divided into three main parts [8]; [9],

$$\frac{d\sigma_{a,xb}(E_a)}{dE_b} = \frac{d\sigma_{a,b}^{SMD}(E_a)}{dE_b} + \frac{d\sigma_{a,b}^{SMC}(E_a)}{dE_b} + \frac{d\sigma_{a,xb}^{MPE}(E_a)}{dE_b} \quad (5)$$

The first term on the right hand side of equation (5) represents the statistical multistep direct (SMD) part which contains from single-step up to five-step contributions. The second term represents the statistical multistep compound (SMC) emission which is based on a master equation. Both terms together (SMD+SMC) represents the first-chance emission process[10][11]. The last term of equation (5) represents the multiple particle emission (MPE) reaction which includes the second-chance, third-chance emissions, etc. These terms are summarized below:

$$\frac{d\sigma_{a,xb}^{MPE}(E_a)}{dE_b} = \sum_c \frac{d\sigma_{a,cb}(E_a)}{dE_b} + \sum_{c,d} \frac{d\sigma_{a,cdb}(E_a)}{dE_b} + \dots \quad (6)$$

2.3 Activation Cross Sections

The following relations between the optical model (OM) reaction cross section and the energy-integrated partial cross sections should be satisfied (at each incident energy (E_a))

$$\sigma_a^{OM} = \sum_b \sigma_{a,b} \quad (7)$$

$$\sigma_{a,b} = \sum_c \sigma_{a,cb} \quad \text{and} \quad \sigma_{a,cb} = \sum_d \sigma_{a,cdb} \quad (8)$$

with $\sigma_{a,b} = \sigma_{a,b}^{SMD} + \sigma_{a,b}^{SMC}$ the total first-chance emission, in this context, activation cross sections are given by

$$\sigma_{a,b\gamma} = \sigma_{a,b} - \sum_{c \neq \gamma} \sigma_{a,cb} \quad (9)$$

$$\sigma_{a,cb\gamma} = \sigma_{a,cb} - \sum_{d \neq \gamma} \sigma_{a,cbd} \quad (10)$$

where $b, c, d \neq \gamma$

For example, the (n,p) -activation cross sections have the form

$$\sigma_{a,p\gamma} = \sigma_{n,p} - \sigma_{n,pn} - \sigma_{n,2p} - \sigma_{n,p\alpha} \quad (11)$$

The SMD cross section is a sum over s -step direct processes given by:[13]

$$\frac{d\sigma_{a,b}^{SMD}(E_a)}{dE_b} = \sum_{s=1} \frac{d\sigma_{a,b}^s(E_a)}{dE_b} \quad (12)$$

The SMD cross section has the form

$$\frac{d\sigma_{a,b}^{SMC}(E_a)}{dE_b} = \sigma_a^{SMC}(E_a) \sum_{N=N_0}^{N^I} \frac{\tau_N(E)}{\hbar} \sum_{(\Delta V)} \Gamma_{N,b}^{(\Delta V)}(E, E_b) \uparrow \dots \quad (13)$$

where τ_N satisfies the time-integrated master equation

$$-\hbar\delta_{NN_0} = \Gamma_{N-2}^{(+)}(E) \downarrow \tau_{N-2}(E) + \Gamma_{N+2}^{(-)}(E) \downarrow \tau_{N+2}(E) - \Gamma_N(E)\tau_N(E) \quad (14)$$

and

$$\Gamma_N^{(\Delta V)}(E) \downarrow = 2\pi I_{SS}^2 \rho_N^{(\Delta V)}(E) \quad (15)$$

The multiple particle emission is expressed as:

$$\frac{d\sigma_{a,xb}^{MPE}(E_a)}{dE_b} = \sum_c \frac{d\sigma_{a,cb}(E_a)}{dE_b} + \sum_{cd} \frac{d\sigma_{a,cdb}(E_a)}{dE_b} + \dots \quad (16)$$

To keep the model tractable, a simple two-body interaction is assumed:[10]

$$I(r_1, r_2) = -4\pi \frac{F_0}{A} [\chi_{nl}(R)]^{-4} \delta(r_1 - r_2) \delta(r_1 - R) \quad (17)$$

$F_0 = 27.5$ MeV taken from nuclear structure considerations[12].

The factor $[\chi_{nl}(R)]^{-4}$ contains the wave function at the nuclear radius $R = r_0 A^{1/3}$

The single-particle state density of particles $C = n, p, \alpha$ with mass μ_c is given by

$$\begin{aligned} \rho(E_c) &= \frac{4\pi V \mu_c (2\mu_c E_c)^{1/2}}{(2\pi\hbar)} \\ &= (4.48 \times 10^{-3} \text{fm}^{-3} \text{MeV}^{-3/2}) r_0^3 A E_c^{1/2} \end{aligned} \quad (18)$$

where $V = \frac{4\pi R^3}{3}$ is equal to the nuclear volume[9].

The single-particle state density of bound particles (at Fermi energy) is then defined by

$$g = 4\rho(E_F) \quad (19)$$

where the factor 4 considers the spin and isospin degeneracy

3. Methodology

The installed EXIFON code on a personal computer was used, which is a computer program package for computational nuclear Data physics which is based on an analytical model for statistical multistep direct and multistep compound reactions (SMD/SMC model). It predicts emission spectra, angular distributions, and activation cross sections for neutrons, protons, alpha particles, and photons. Multiple particle emissions are considered for up to three decays of the compound system.

The model is based on random matrix physics with the use of the Green's function formalism[13];[14]. All calculations are performed without any free parameters. Cross-section Results were obtained for bombarding energies below 30 MeV[15];[16].

3.1 Shell structure Effects

The shell structure effects are considered in SMC processes. Under such a situation, the single-particle state density g , in equation (2.17) is multiplied by the factors

$$\left(1 + \frac{\delta W}{E_x} [1 - \exp\left\{-\frac{\delta W}{E_x} - \gamma E_x\right\}] \right) \quad (20)$$

With $\gamma = 0.05 \text{MeV}^{-1}$ and δW as the shell correction energy taken from tables[17].where the quantity $E_x = E$ or U which denotes the excitation energy of the composite or residual systems respectively.

The calculations in this study were performed with ($\delta W \neq 0$) and without ($\delta W = 0$) shell corrections.

4. Results and Discursions

The interaction cross section was obtained and tabulated in table 1 for neutron as incident particle. Which is then plotted the cross section against energy in Figures 1 to 6 in order to see the behavior graphically. The calculations in which the shell correction was taken into consideration are denoted by 'With shell correction' on the graph's legend, while those without the shell correction effects are denoted by 'Without shell correction'.

Table 1. The Cross section obtained from the reactions with shell correction and reactions without shell correction at each particular energy ranges from (0-30)MeV on target nucleus ^{208}Bi .

with shell correction					without shell correction			
Energy	(n,a)	(n,na)	(n,ag)	(n,an)	(n,a)	(n,na)	(n,ag)	(n,an)
1	0	0	0	0	0	0	0	0
2	0	0	0	0	0	0	0	0
3	0	0	0	0	0	0	0	0
4	0	0	0	0	0	0	0	0
5	0	0	0	0	0	0	0	0
6	0	0	0	0	0	0	0	0
7	0	0	0	0	0	0	0	0
8	0	0	0	0	0	0	0	0
9	0	0	0	0	0	0	0	0
10	0	0	0	0	0	0	0	0
11	0	0	0	0	0	0	0	0
12	0	0	0	0	0	0	0	0
13	0	0	0	0	0	0	0	0
14	0	0	0	0	0	0	0	0
15	0	0	0	0	0	0	0	0
16	0	0	0	0	0	0	0	0
17	0.1	0	0	0	0	0	0	0
18	0.1	0	0	0	0.1	0	0	0
19	0.1	0	0	0.1	0.1	0	0	0.1
20	0.2	0.1	0	0.1	0.1	0.1	0	0.1
21	0.2	0.2	0	0.2	0.2	0.1	0	0.1
22	0.3	0.2	0	0.3	0.2	0.2	0	0.2
23	0.4	0.4	0	0.3	0.3	0.3	0	0.3
24	0.5	0.5	0	0.4	0.4	0.4	0	0.3
25	0.5	0.6	0	0.5	0.4	0.5	0	0.4
26	0.6	0.8	0	0.6	0.5	0.7	0	0.5
27	0.7	1	0	0.7	0.6	0.8	0	0.6
28	0.8	1.2	0	0.7	0.7	1	0	0.6
29	0.8	1.4	0	0.8	0.7	1.2	0	0.7
30	0.9	4.1	0	0.9	0.8	3.9	0	0.8

with shell correction					without shell correction			
Energy (MeV)	(n,p)	(n,np)	(n,2p)	(n,2np)	(n,p)	(n,np)	(n,2p)	(n,2np)
1	0	0	0	0	0	0	0	0
2	0	0	0	0	0	0	0	0
3	0	0	0	0	0	0	0	0
4	0	0	0	0	0	0	0	0
5	0	0	0	0	0	0	0	0
6	0.1	0	0	0	0	0	0	0
7	0.3	0	0	0	0.1	0	0	0
8	0.7	0	0	0	0.3	0	0	0
9	1.4	0	0	0	0.7	0	0	0
10	2.4	0	0	0	1.3	0	0	0
11	4	0	0	0	2.4	0	0	0
12	6	0	0	0	3.9	0	0	0
13	8.5	0	0	0	5.9	0	0	0
14	11.5	0	0	0	8.4	0	0	0
15	14.8	0.1	0	0	11.3	0	0	0
16	18.4	0.2	0	0	14.6	0.1	0	0
17	22.3	0.3	0	0	18.3	0.1	0	0
18	26.4	0.4	0	0	22.1	0.2	0	0
19	30.7	0.6	0	0	26.2	0.3	0	0
20	35.1	0.8	0	0	30.5	0.5	0	0
21	39.6	1.1	0	0	34.9	0.7	0	0
22	44.3	1.4	0	0	39.5	1	0	0
23	49	1.7	0	0.1	44.1	1.3	0	0
24	53.8	2.1	0	0.2	48.9	1.7	0	0.1
25	58.8	2.5	0	0.3	53.8	2.1	0	0.1
26	63.7	2.9	0	0.4	58.8	2.5	0	0.2
27	68.8	3.4	0	0.6	63.8	3	0	0.4
28	73.9	3.8	0	0.9	68.9	3.5	0	0.6
29	79.1	4.2	0	1.2	74	4	0	0.9
30	84.3	4.7	0	1.6	79.2	4.5	0	1.2

4.1 Production of Lead Isotopes

In figure 1: $^{208}\text{Bi}(n, p)^{208}\text{Pb}$ is charge exchange reactions were by the incident neutron displaced proton from the nucleus of the bismuth forming nucleus of ^{208}Pb isotope. The reaction cross section increases with increase in energy around 8 MeV, This shows that production of ^{208}Pb through this route is possible at this energy range.

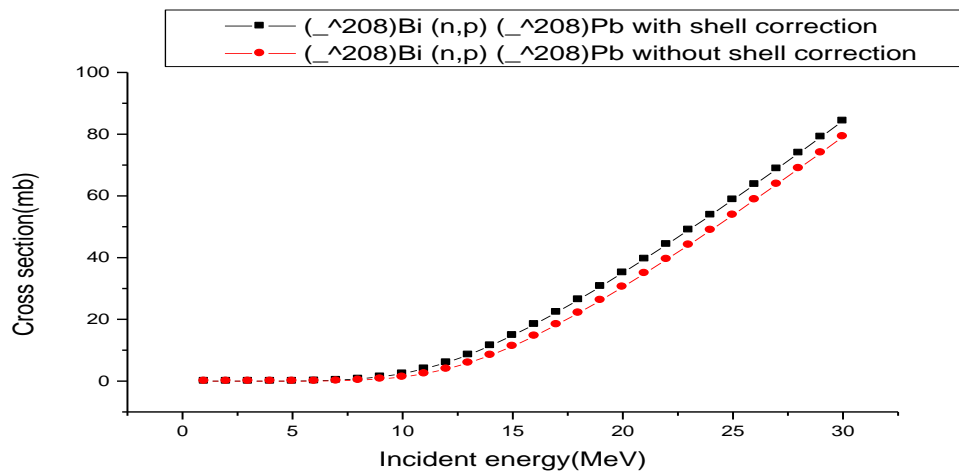


Figure 1: graph of cross section against incident energy for the $^{208}\text{Bi}(n, p)^{208}\text{Pb}$ reaction

The Figure 2 $^{208}\text{Bi}(n, np)^{207}\text{Pb}$ reaction is The knock out reaction in which the reaction cross section increases with increase in energy at the range 0 MeV to 30 MeV, the reaction without shell correction has a maximum cross section around 1.4mb. While when the shell correction was considered the maximum value of cross section increased to 1.7mb. This show that shell correction affect the values of the cross section in this reaction.

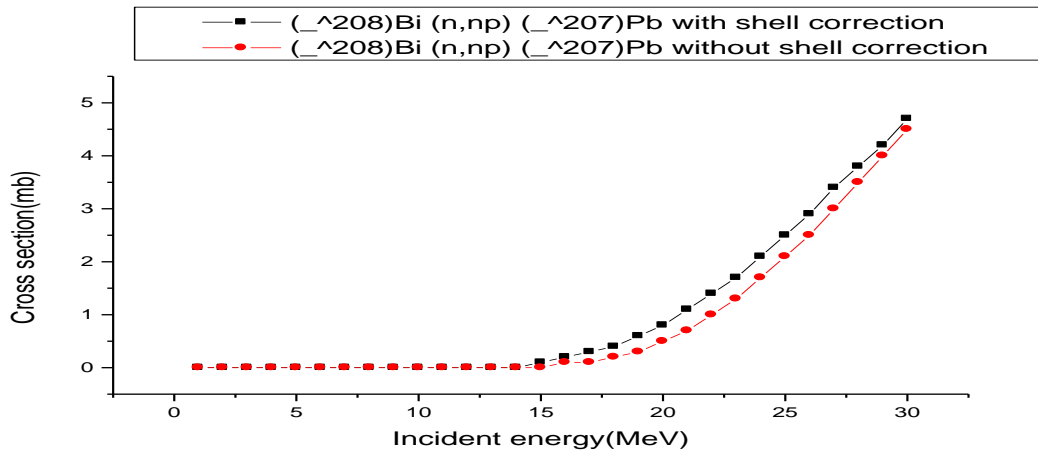


Figure 2:graph of cross section against incident energy for the $^{208}\text{Bi}(n,np)^{207}\text{Pb}$ reaction

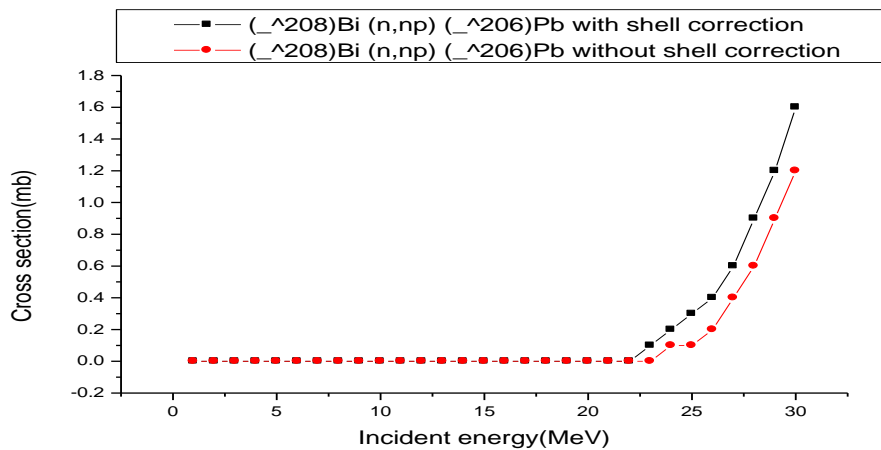


Figure 3:graph of cross section against incident energy for the $^{208}\text{Bi}(n,2np)^{206}\text{Pb}$ reaction

4.2 Production of Thallium Isotopes

Production of ^{207}Tl Isotope

^{207}Tl is an isotope of thallium with half-life of 4.76 minutes and it decays via beta (^-e) or gamma particles. The $^{208}\text{Bi}(n,2p)^{207}\text{Tl}$ is a knock out reaction where 2 protons are emitted and produce ^{207}Tl . This type of reaction is not observed because the cross section is zero throughout the energy range we considered in the table above, introducing the shell correction does not change anything to the results. This shows that production of ^{207}Tl through this route is not possible at this energy range.

Production of ^{205}Tl isotope

^{205}Tl is a stable isotope of thallium, the $^{208}\text{Bi}(n,a)^{205}\text{Tl}$ reaction is the knock out reaction in which the cross section increases with increase in energy at the range 0 MeV to 30 MeV, the reaction without shell correction has a maximum cross section around 0.8mb. While when the shell correction was considered the maximum value of cross section increased to 0.9mb. This shows that shell correction effect affects the value of the cross section in this reaction.

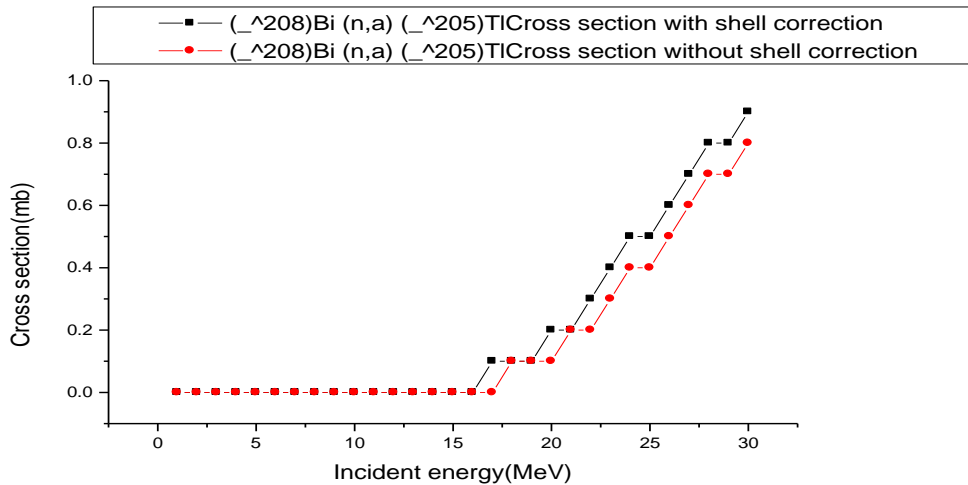


Figure 4: graph of cross section against incident energy for the: $^{208}\text{Bi}(n, a)^{205}\text{Tl}$ reaction

The $^{208}\text{Bi}(n, ag)^{205}\text{Tl}$ reaction is the knock out reaction. This type of reaction was not observed because the cross section is zero throughout the energy range considered in table 1, introducing the shell correction does not change anything to the results. This shows that production of ^{205}Tl through this route is not possible at this energy range.

Production of ^{204}Tl isotope

^{204}Tl is an isotope of thallium with half-life of 2.7 years and it decays via beta(^-e) or K-capture, the $^{208}\text{Bi}(n, na)^{208*}\text{Bi} \rightarrow ^{204}\text{Tl}$ reaction is inelastic scattering followed by knock out reaction where an alpha particle is emitted and produced ^{204}Tl . Reaction without shell correction has maximum cross section around 3.9mb, when the shell correction was considered the maximum value of cross section increased to 4.1mb

Figure 4.5: $^{208}\text{Bi}(n, an)^{205}\text{Tl} \rightarrow ^{204}\text{Tl}$ reaction is a knock out reaction where alpha particle is emitted and produced ^{205}Tl which is unstable nucleus and decays by emitting neutron to form ^{204}Tl . Reaction without shell correction has maximum cross section of 0.8mb. When the shell correction was considered the maximum value of cross section increased to 0.9 mb. So $^{208}\text{Bi}(n, na)^{208*}\text{Bi} \rightarrow ^{204}\text{Tl}$ is a best route for production of ^{204}Tl with cross section of 4.1mb.

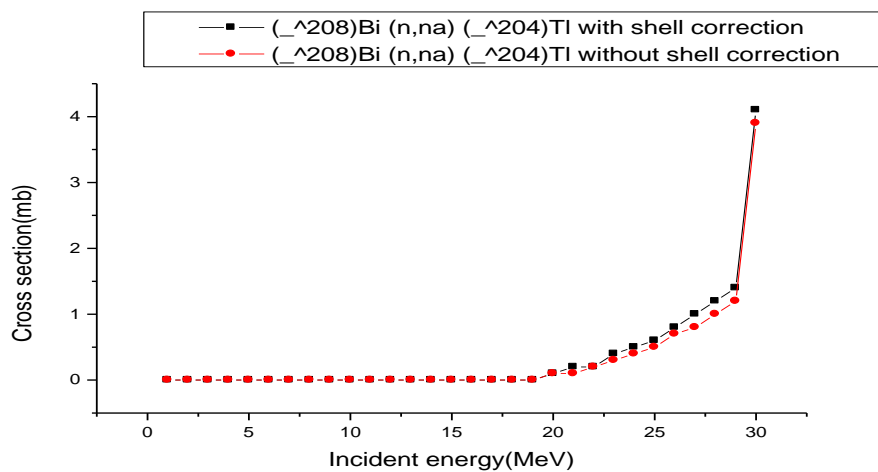


Figure 5: graph of cross section against incident energy for the $^{208}\text{Bi}(n, na)^{208*}\text{Bi} \rightarrow ^{204}\text{Tl}$ reaction

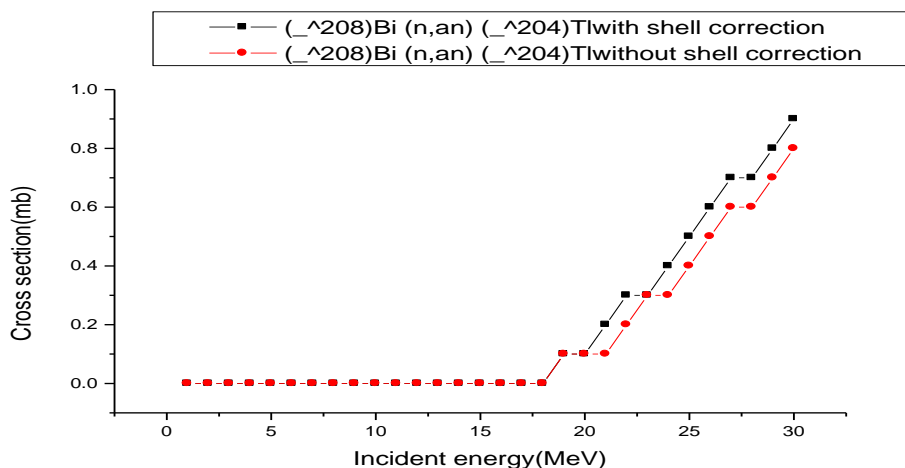


Figure 6: graph of cross section against incident energy in the $^{208}\text{Bi}(n, an)^{205}\text{Tl} \rightarrow ^{204}\text{Tl}$ reaction

5. Conclusions

Precise knowledge of the reactions cross-section is needed in radionuclide production. Nuclear reactions were studied and evaluated the cross section for the production of isotopes of thallium and lead using EXIFON code. Our results show that production of ^{207}Tl is not observe through $^{208}\text{Bi}(n, 2p)^{207}\text{Tl}$ reaction and also production of ^{205}Tl through $^{208}\text{Bi}(n, ag)^{205}\text{Tl}$ route is not possible at considered energy range.

The reaction cross section for the production of ^{208}Pb , ^{207}Pb , ^{206}Pb , ^{205}Tl and ^{204}Tl through $^{208}\text{Bi}(n, p)^{208}\text{Pb}$, $^{208}\text{Bi}(n, p)^{208}\text{Pb}$, $^{208}\text{Bi}(n, a)^{205}\text{Tl}$, $^{208}\text{Bi}(n, na)^{208}\text{Bi} \rightarrow ^{204}\text{Tl}$ and $^{208}\text{Bi}(n, an)^{205}\text{Tl} \rightarrow ^{204}\text{Tl}$ were obtained respectively.

This studied show that EXIFON code is a good tool for investigation of nuclear reaction cross section and this research work can be useful in the production of radionuclide of high purity and in an efficient manner for therapeutic purposes embracing current and possible future needs.

References

- [1] S. C. Srivastava, "Therapeutic radionuclides: making the right choice," pp. 63–79, 1996.
- [2] K. Kettern, H. H. Coenen, and S. M. Ā. Qaim, "Quantification of radiation dose from short-lived positron emitters formed in human tissue under proton therapy conditions," vol. 78, pp. 380–385, 2009.
- [3] K. Abusaleem, "Nuclear Data Sheets for," *Nucl. Data Sheets*, vol. 116, pp. 163–262, 2014.
- [4] E. Browne and J. K. Tuli, "Nuclear Data Sheets for A = 137," *Nucl. Data Sheets*, vol. 108, no. 10, pp. 2173–2318, 2007.
- [5] E. Browne and J. K. Tuli, "Nuclear Data Sheets for A = 99," *Nucl. Data Sheets*, vol. 112, no. 2, pp. 275–446, 2011.
- [6] E. Browne and J. K. Tuli, "Nuclear Data Sheets for A = 99," *Nucl. Data Sheets*, vol. 112, no. 2, pp. 275–446, 2011.
- [7] D. Polster and H. Kalka, "Short note Fission within a statistical multistep model," vol. 424, pp. 423–424, 1991.
- [8] B. C. Nesaraja, K. Linse, S. Spellerberg, S. Sudar, A. Suhaimi, and S. M. Qaim, "Excitation Functions of Neutron Induced Reactions on some Isotopes of Zinc , Gallium and Germanium in the Energy Range of 6 . 2 to 12 . 4 MeV," vol. 9, pp. 1–9, 1999.

- [9] Y. E. C. B. F. Ebiwonjumi, "Determination of Nuclear Reaction Cross-sections for Neutron- Induced Reactions in Some Odd – A Nuclides," vol. 32, pp. 55–69, 2014.
- [10] H. Kalka, "Hadrons and Nuclei Statistical multistep reactions from 1 to 100 MeV," vol. 299, pp. 289–299, 1992.
- [11] A. V. M. Rao and J. R. Rao, "Pre-Equilibrium Analysis of the Excitation Functions of (a, xn) Reactions on Silver and Holmium .," vol. 104, pp. 863–874, 1991.
- [12] S. M. Qaim, "The emission of α -particles in 14 MeV neutron induced reactions has been extensively investigated over the last 30 years I). In early studies the nuclear emulsion technique of the processes other than (n, a) are relatively small , the technique , da ," vol. 458, pp. 237–245, 1986.
- [13] K. Muhammed, M. Y. Onimisi, and S. A. Jonah, "Investigation of the Shell Effect on Neutron Induced Cross Section of Actinides," vol. 1, no. 1, pp. 6–9, 2011.
- [14] Y. Watanabe, T. Fukahori, K. Kosako, N. Shigyo, T. Murata, N. Yamano, T. Hino, K. Maki, H. Nakashima, N. Odano, and S. Chiba, "Nuclear Data Evaluations for JENDL High-Energy File," pp. 326–331, 2005.
- [15] H. Ford, "Radiation Safety Information Computational Center CHANGES TO THE RSICC CODE AND," pp. 1–13, 2012.
- [16] J. E. White, J. B. Manneschildt, S. Y. Finch, and J. K. Dickens, "ABSTRACTS OF COMPUTER PROGRAMS AND DATA LIBRARIES PERTAINING TO PHOTON PRODUCTION DATA," *Comput. Phys. Eng. Div.*, 1997.
- [17] S. Yamoah and M. Asamoah, "Calculations of Excitation Functions of (n, p), (n, a) and ($n, 2n$) Reaction Cross-Sections for Stable Isotopes of from Reaction Threshold to 20 MeV," vol. 3, no. 4, pp. 100–107, 2013.